ELSEVIER

Polymer 43 (2002) 4269–4275

polymer

www.elsevier.com/locate/polymer

Energetic analysis of the two PMMA chain tacticities and PMA through molecular dynamics simulations

Armand Soldera

Département de Chimie, Université de Sherbrooke, Sherbrooke, Que., Canada J1K 2R1

Received 13 September 2001; received in revised form 12 February 2002; accepted 12 February 2002

Abstract

Simulated dilatometry techniques have been applied to compute the glass transition temperatures, T_gs, of the two poly(methyl methacrylate) (PMMA) chain tacticities, and poly(methyl acrylate) (PMA). Since the difference in T_gs between the two configurations was accurately simulated, further analysis could be carried out. This article more particularly deals with energetic and structural analysis of the difference. Thus this analysis showed that the non-bond energy and the bending angle energy associated with the intradiad backbone angle, principally contribute to the energetic difference between the two PMMA configurations. Following the free volume theory, these two energetic variations allow an increase in T_g in comparison to PMA, and an enlargement of the difference in the T_gs between the two PMMA configurations. Actually, these two energetic contributions stem from the substitution of the hydrogen atom attached to the chiral carbon atom in the PMA repeat unit by a methyl group. The same behavior is encountered with the two poly(ethyl methacrylate) (PEMA) chain tacticities.

Keywords: Poly(ethyl methacrylate); Glass transition; *pcff*

1. Introduction

Understanding the glass transition is a long-standing issue in both the industry and academic sectors. Numerous experimental techniques coupled with advanced theories have been used towards this end [1,2]. With molecular modeling, a supplementary way of investigation has emerged [3]. The matter can thus be probed to interpret the reasons that give rise to the macroscopic properties. From a molecular simulation vision of the glass transition, poly(methyl methacrylate) (PMMA) provides a real center of interest since the difference in the glass transition temperatures, T_gs, between the two chain tacticities might be interpreted only in terms of changes in molecular characteristics. In a previous work [4], the glass transitions of the two PMMA chain tacticities have been simulated. The difference in the simulated T_gs between the two PMMA configurations was found to be consistent with the experimental value. From a simulation viewpoint, the interactions between atoms are therefore accurately expressed. Investigations to explain the difference in T_gs can be carried out using data stemming from simulation. In this study, the time step has been extended and the number of configurations increased compared to the previous work [4], in order to refine the results obtained from the simulation. Moreover, since no tacticity dependence on T_g is experimentally observed when the methyl group linked to the backbone chain is substituted by an hydrogen atom, the two poly(methyl acrylate) (PMA) configurations obtained have been simulated. The energetic and structural variation brought by the presence or not of the methyl group can then be regarded. To confirm the results derived from this analysis, the two chain tacticities of poly(ethyl methacrylate) (PEMA) have also been simulated.

2. Simulation description

The syndiotactic and isotactic PMMA will be denoted s-PMMA and i-PMMA, respectively. The structural unit is displayed in Fig. 1.

2.1. Simulation

All the simulations have been performed using the periodic boundary conditions [5]. The polymer chains, with one hundred repeat units, propagate into the periodic box according to the self-avoiding walk technique [6] with the long-range non-bonded interactions described by Theodorou and Suter [7]. The procedure is implemented in the MSI *Amorphous_Cell*© software. To get the T_g, the

E-mail address: armand.soldera@courrier.usherb.ca (A. Soldera).

0032-3861/02/$ - see front matter
PII: S0032-3861(02)00240-9

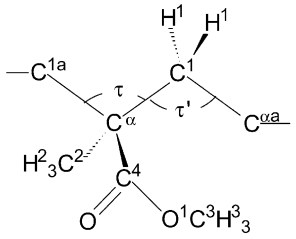

Fig. 1. Structural unit of PMMA. The superscript letters indicate the position of atoms. The τ and τ' angles correspond to the notation used by Vacatello and Flory [25].

simulated dilatometry technique is employed [8]. As in the experimental dilatometry technique, the specific volume, i.e. the inverse of the density, is reported versus the temperature. The intercept of the lines joining the points of the two phases, the vitreous and rubbery, yields the value of the T_g. In order to acquire the density at a desired temperature, molecular dynamics (MD) simulations are performed in the NPT statistical ensemble, i.e. constant number of particles, pressure and temperature. The simulated density directly comes from the knowledge of the periodic box volume. The pressure is controlled according to the Parrinello–Rahman algorithm [9], while the temperature is imposed, in the primary step by the velocity scaling algorithm, and then through the Andersen algorithm [10]. The integration step is 0.001 ps using the Verlet-leap frog algorithm [11]. The simulated cooling rate is indeed extremely rapid, in order of 10^9 times more rapid than an experimental quenching rate. Consequently, due to the 'time–temperature superposition principle', higher values of the T_gs compared to the experimental ones are reported [12].

During the previous studies, the simulation time for one data was 0.1 ns [4]. Configurations at 307, 267, 247, 227, 167, 127, 67 and 27 °C, were kept, and are used in the present study, with a prolonged MD simulation time of 1 ns at the corresponding temperature. Configurations are saved every 0.5 ps. To accurately represent the molecular behavior, four additional MD simulations at 67 and 227 °C have been carried out according to the procedure described by Fried [13]. The same procedure has been applied at 67 °C for both chain tacticities of PEMA.

2.2. Force field

All the calculations were performed using an empirical force field [14] since relatively large systems were studied, and the computation of T_g implies long time periods [12]. To adequately express the interaction between atoms inside a polymer, a force field has to possess at least a non-bond, or intermolecular, and an intramolecular contribution:

$$V = V_{\text{non-bond}} + V_{\text{intramolecular}} \tag{1}$$

The two terms on the right-hand side of Eq. (1) can be split into specific contributions that are actual mathematical translations of specific interactions. The non-bond energy function expresses interactions between atoms that are not bonded to each other; it is generally separated into a van der Waals, the steric component, and a Coulombic, the electrostatic component, terms

$$V_{\text{non-bond}} = V_{\text{vdW}} + V_{\text{Coulombic}} \tag{2}$$

with

$$V_{\text{vdW}} = \frac{A_{ij}}{r_{ij}^n} - \frac{B_{ij}}{r_{ij}^6}, \qquad V_{\text{Coulomb}} = \frac{q_i q_j}{\varepsilon r_{ij}}$$

In these equations, r_{ij} denotes the distance between atoms i and j; ε is the dielectric constant; q_i is the partial charges of atom i [5]; and A_{ij} and B_{ij} are deduced from the usual Lennard–Jones parameters, when $n = 12$, applying the Lorentz–Berthelot mixing rules [5]. q_i, A_{ij}, and B_{ij} are provided by the employed force field. The parameter n varies according to the force field. An r^{-9} power repulsion term seems to allow more accurate calculations [15]. Such a 9–6 form for the van der Waals interaction is employed in the *pcff* force field used during this study [16].[1] It has to be pointed out that using this force field systematic errors in the pressure–volume–temperature relation determination have been reported [17]. Moreover, *pcff* tends to underestimate densities. However, according to the procedure exposed in Section 3.1, relative densities of both configurations are accurately simulated. At 298 K, experimental densities of i-PMMA and s-PMMA are 1.22 and 1.19 g cm^{-3} [18], respectively, while the simulated densities are found to be 1.10 and 1.05 g cm^{-3} for iso- and syndiotactic configurations, respectively. Finally *pcff* has shown its efficiency in correctly describing the difference in T_gs between the two PMMA configurations [4]. Consequently, energetic and structural investigations on such a difference can be carried out using this force field.

In its simplest form, the intramolecular energy function is split into a connectivity term, the bond stretching function, and flexibility terms, the angle bending and the torsional functions. For *pcff* the bond stretching and angle bending terms are quartic functions, while the torsion term is a three-term Fourier expansion

$$V_{\text{intramolecular}} = V_{\text{bond}} + V_{\text{angle}} + V_{\text{torsion}} \tag{3}$$

with

$$V_{\text{bond}} = k_2(r - r_0)^2 + k_3(r - r_0)^3 + k_4(r - r_0)^4,$$

$$V_{\text{angle}} = h_2(\theta - \theta_0)^2 + h_3(\theta - \theta_0)^3 + h_4(\theta - \theta_0)^4,$$

$$V_{\text{torsion}} = V_1\left[1 - \cos\left(\phi - \phi_1^0\right)\right] + V_2\left[1 - \cos\left(2\phi - \phi_2^0\right)\right] + V_3\left[1 - \cos\left(3\phi - \phi_3^0\right)\right]$$

k_2, k_3, k_4, h_2, h_3, h_4, V_1, V_2, V_3, r_0, θ_0, ϕ_1^0, ϕ_2^0, and ϕ_3^0, are potential parameters. Potential parameters that are relevant

[1] Discover_3® from Molecular Simulation Inc.

Table 1
pcff parameters relevant for the study (the AMBER atom type convention is employed: CT = sp^3 carbon, C = carbonyl carbon, HC = hydrogen attached to carbon, O = carbonyl oxygen, OS = ethyl and ester oxygen)

Bonds	X_0 (Å)	k_2 (kcal mol^{-1} Å^{-2})	k_3 (kcal mol^{-1} Å^{-3})	k_4 (kcal mol^{-1} Å^{-4})
CT–CT	1.53	299.67	−501.77	679.81
Angles	θ_0 (deg)	h_2 (kcal mol^{-1} deg^{-2})	h_3 (kcal mol^{-1} deg^{-3})	h_4 (kcal mol^{-1} deg^{-4})
CT–CT–CT	112.67	39.516	−7.443	−9.5583
CT–CT–C	108.53	51.9747	−9.4851	−10.9985
HC–CT–HC	107.66	39.641	−12.921	−2.4318
CT–CT–HC	110.77	41.453	−10.604	5.129
CT–C–O	123.145	55.5431	−17.2123	0.1348
CT–C–OS	100.318	38.8631	−3.8323	−7.9802
O–C–OS	120.797	95.3446	−32.2869	6.3778
C–OS–CT	113.288	61.2868	−28.9786	7.9929
OS–CT–HC	107.688	65.4801	−10.3498	5.8866

for this work are presented in Table 1. r, θ, and ϕ, correspond to the internal coordinates: distance, valence angle, and dihedral bonds, respectively. Using a BTCL program,[1] they can be extracted from configuration files.

The construction of a force field implies that individual contributions to the energy expression are linearly related. However, meaningful results can be obtained from comparing energies of structurally different molecules if they contain the same number and types of structural units [19]. Since the two configurations of PMMA have exactly the same force field parameters, changes in their energetic behavior will directly be linked to changes in their molecular characteristics. In fact, the study with the two PMMA configurations, showed that each energetic function, as described in previous equations, has its proper physical significance and can be looked at separately from the other contributions. Considering a particular internal parameter, the computation of the associated energetic function for both configurations can thus give insight into the difference in molecular behavior associated to this internal parameter. Moreover, the non-bond terms in PMA and PMMA, can also be distinguished in order to examine the intermolecular contribution brought by the substitution of the hydrogen atom by a methyl group. Comparing internal energetic terms between these two polymers could not be carried out since the number of internal coordinates is different. In fact, the variation of each internal coordinate can be determined from a trajectory file. Inasmuch as the specific potential parameters (Table 1) and the potential functions (Eqs. (1)–(3)) are known, the energy associated to the considered internal coordinate can be computed. Its contribution to the average energy can thus be established. Actually, such a calculation is carried out according to the following equation

$$\langle V \rangle = \frac{1}{Nt} \sum_{i=1}^{N} \sum_{j=1}^{t} V_i(j)$$

where $V_i(j)$ is the potential energy computed from the value of the internal parameter i at time j of the simulation following Eq. (3); N is the number of repeat units along one polymer chain; t is the number of configurations saved during an MD simulation; and the brackets denote both the averages in time and along the backbone chain.

It has to be pointed out that *pcff* contains, in addition to the five terms of Eqs. (1)–(3), an out-of-plane term and numerous cross-terms. The introduction of these supplementary terms makes this force field especially useful to represent vibrational spectra [20] with a good accuracy and allows to work with a great number of polymers. Actually, since these terms do not intervene much in the total energy, they were not considered in this paper.

3. Results and discussion

3.1. Simulated dilatometry

The specific volumes with respect to temperatures are plotted in Fig. 2 for the two PMMA configurations. The difference in the T_gs between the two PMMA configurations, 60 °C, is in accordance with the experimental data, 73 °C. Consequently, microscopic interactions are correctly simulated, and further investigations on the energetic difference between the two configurations can be carried out.

The substitution of the attached backbone methyl group in PMMA by an hydrogen atom gives PMA. From experimental data, the isotactic and syndiotactic PMA chains exhibit very close T_gs, both in order of 10 °C [21]. Fig. 3 shows the simulated dilatometric data for the two PMA configurations. The simulated T_gs, 120 °C, are comparable for both PMA configurations. Consequently, the two PMA chain tacticities were combined to present the following results and discussion. Using dilatometric simulation technique, the difference between the T_gs of i-PMMA and PMA is 37 °C, while the experimental difference is 40 °C. Independently of the values of the T_gs, the difference is

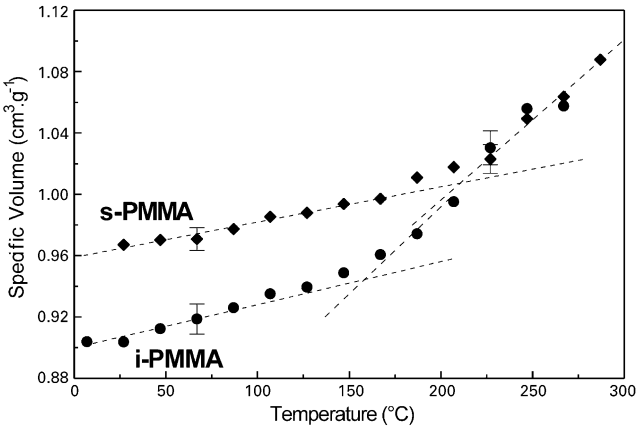

Fig. 2. The specific volumes of i-PMMA (●) and s-PMMA (◆) are plotted versus temperature. T_g is determined by the intersection of the regression fit lines (- - -) of the two phases. For clarity, only standard deviations at 67 and 227 °C are presented.

correctly simulated, i.e. the T_g of PMA is below that of i-PMMA in the same order of magnitude as in experimental data. Differentiation between PMMA and PMA can then be performed through an energetic analysis.

3.2. Energetic differences

Energetic behaviors between polymer chains are primary compared at one temperature, 67 °C. This temperature corresponds to the glassy state for all the studied polymers. Table 2 displays the differences in the energetic contributions (Eqs. (1)–(3)) between the two PMMA configurations, at this temperature. A positive value indicates that the computed energy for i-PMMA is higher than that of s-PMMA. The syndiotactic configuration exhibits lower total and intramolecular energies than the isotactic configuration but it presents a higher non-bond energy. These behaviors are in accordance with published data [4].

The values of the non-bond energy by monomer at 67 °C for s-PMMA, i-PMMA and PMA, are 350 (±10), 258

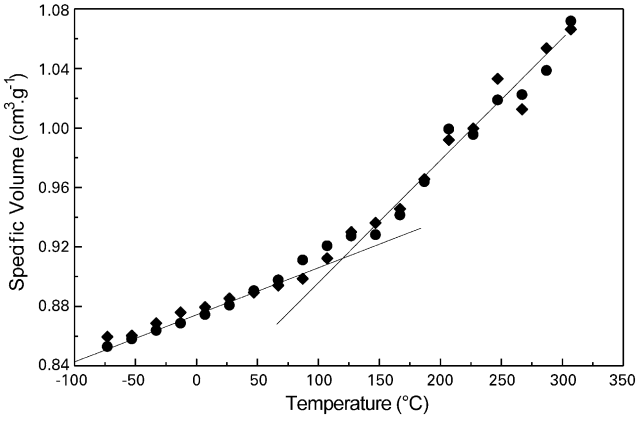

Fig. 3. The specific volumes of isotactic (●) and syndiotactic (◆) PMA are plotted against temperature. T_g is determined by the intersection of the regression fit lines (—) of the two phases.

Table 2
Differences in main energy contributions between the two PMMA chain tacticities at 67 °C. A positive value indicates that the corresponding energy of i-PMMA is higher than that of s-PMMA

Energy contribution	Difference (kcal mol^{-1})
Total energy	10 (±6)
Intermolecular energy	−35 (±8)
Intramolecular energy	45 (±8)
Stretching energy	15 (±7)
Angle energy	75 (±10)
Dihedral energy	15 (±5)

(±10), and 78 (±10) kcal mol^{-1}, respectively. Following the free volume theory, higher interactions between neighboring polymer chain segments will give a higher T_g. Actually, to allow a cooperative motion of polymer chain, holes of sufficient size have to be created. As a matter of fact, greater are the interchain interactions, greater is the thermal energy brought to the system in order for the phenomenon to occur; hence greater is the T_g. The reported non-bond energies involve that the T_g(s-PMMA) is higher than T_g(i-PMMA) which is higher than T_g(PMA). Such a distinction is in accordance with the values of the experimental and simulated T_gs of the three polymers. The introduction of the methyl group thus brings major interactions between PMMA chains that yields to an increase in the T_g. However, the difference between the two PMMA configurations is too important to only be attributed to a difference in the intermolecular interactions. To corroborate this fact, two points have to be emphasized. Firstly, the computation of the T_g by a QSPR [22] method gives a value of 84 °C, for both PMMA configurations, while a value of 34 °C was computed for PMA. Since the tacticity is not taken into account with this method, the computed value can be considered as the 'expected' T_g for PMMA, analogous to the T_g of atactic-PMMA. According to these results, the experimental T_g(i-PMMA), 50 °C, and T_g(s-PMMA), 123 °C, are lower and higher, respectively, than the expected T_g. Secondly, the difference between the two PMMA configurations of the intramolecular energy is higher than the difference in the non-bond energy, leading to the highest total energy for i-PMMA (Table 2). Inspecting the intramolecular contribution differences between the two PMMA configurations in Table 2, the difference in the angle bending term is clearly most significant. In order to find which angle contributes the most to the difference in the total angle bending energy, the energy associated to each valence angle (28 by monomer) of both PMMA chains is computed according to the procedure previously described. It has to be pointed out that the difference in the torsional energy between the two PMMA configurations is low. As a matter of fact, this term does not contribute much to the differentiation of the T_gs through an energetic analysis, although it intervenes in the values of the T_gs by the magnitude of its torsional barriers [23].

All the angle bending energies, the corresponding

Table 3
Angle bending energies by monomer, and the corresponding average angle, associated to all the valence angles of the two PMMA chain tacticities, and their difference, at 67 °C. The atom names are the same as those shown in Fig. 1 (the asterisk refers to a hydrogen atom different from the first one but attached to the same carbon atom)

Angle	i-PMMA kcal mol^{-1} (°)	s-PMMA kcal mol^{-1} (°)	Difference kcal mol^{-1} (°)
C^{α}–C^{1}–C^{α}	2.70 (127.8)	2.36 (126.6)	0.34 (1.3)
C^{α}–C^{1}–H^{1} (2^{a})	0.74 (104.6)	0.56 (105.8)	0.18 (−1.2)
C^{2}–C^{α}–C^{1}	0.39 (110.9)	0.30 (111.4)	0.09 (−0.5)
C^{α}–C^{1}–H^{2} (2^{a})	0.48 (106.4)	0.54 (106.0)	− 0.06 (0.4)
C^{α}–C^{4}–O^{1}	1.65 (111.9)	1.69 (112.0)	− 0.04 (0.1)
C^{4}–C^{α}–$C^{1'}$	0.28 (109.2)	0.25 (108.6)	0.03 (0.6)
$\tau(C^{1}$–C^{α}–$C^{1'})$	0.82 (106.7)	0.80 (106.6)	0.02 (0.1)
C^{2}–C^{α}–$C^{1'}$	0.39 (110.5)	0.37 (110.9)	0.02 (−0.4)
H^{1}–C^{1}–H^{1*}	0.48 (103.9)	0.47 (104.0)	0.01 (−0.1)
C^{1}–C^{α}–C^{4}	0.28 (109.0)	0.27 (108.5)	0.01 (0.5)
C^{α}–C^{4}–O	0.27 (125.4)	0.26 (125.2)	0.01 (0.2)
H^{2}–C^{2}–H^{2*} (3^{a})	0.31 (107.0)	0.30 (107.0)	0.01 (0.0)
C^{α}–C^{2}–H^{2} (3^{a})	0.30 (111.7)	0.29 (111.6)	0.01 (0.1)
O^{1}–C^{3}–H^{3} (3^{a})	0.39 (109.5)	0.39 (109.5)	0 (0.0)
C^{2}–C^{α}–C^{4}	0.29 (109.8)	0.29 (110.4)	0 (−0.6)
C^{4}–O^{1}–C^{3}	0.9 (119.4)	0.9 (119.4)	0 (0.0)
O^{1}–C^{4}–O	0.33 (122.5)	0.33 (122.5)	0 (0.0)
H^{3}–C^{3}–H^{3*} (3^{a})	0.30 (109.3)	0.30 (109.3)	0 (0.0)

[a] The number corresponds to the number of equivalent energetic terms associated with the angle. The associated energy has to be multiplied by this number.

average angle, of the two PMMA configurations, as well as their difference, are reported in Table 3. A positive difference value corresponds to a higher energy for the associated angle in the isotactic configuration. The sum over all the differences gives 0.74 kcal mol^{-1}, which corresponds to the actual difference in the valence energy associated to one monomer. Since the studied polymers have one hundred monomers, the difference is in accordance with the value directly obtained from the simulation, 75 kcal mol^{-1} (Table 2). From Table 3, it is observed that the major energy contribution comes from the intradiad backbone angle τ' (Fig. 1). As a matter of fact, the variation of this angle with respect to temperature is considered for the two PMMA configurations and for PMA. These variations are reported in Fig. 4. Comparable temperature behaviors are observed for each intradiad angle of the three polymers. The great reported energies (Table 3) originate from the gap between the expected value for such an angle, 112.67°, assigned by the force field (Table 1), and the values derived from the MD simulations: 127.8° (±0.1°), 126.7° (±0.1°), and 118.0° (±0.1°), at 67 °C, for the isotactic and syndiotactic PMMA configurations, and PMA, respectively. According to Vacatello and Flory [24], this angle opens to lessen the repulsive interactions between the side groups. A low value for PMA confirms the role of the methyl group in the aperture of the intradiad backbone angle. Such a steric adjustment is also revealed by an extension of the carbon–carbon distance along the backbone chain: for the PMA, it is 1.56 Å (±0.02 Å) while for both PMMA configurations, it is slightly superior, 1.59 Å (±0.02 Å). However, in the case of the valence angle, the opening varies according to the tacticity of the PMMA chains. The introduction of an ether group along a backbone chain tends to decrease the T_g of the polymer due to an increase in the chain flexibility brought by an aperture of the backbone angle [25]. The methyl group greatly opens the intradiad backbone angle of PMMA compared to PMA, but due to the important non-bond interactions, T_gs of PMMA are higher than the T_g of PMA. However, a higher value of τ' for i-PMMA, and therefore a greater mobility for its chains, is in accordance with its lower T_g compared with T_g(s-PMMA). The other major contributions to the valence angle energy come from the angles that make the hydrogen–carbon bonds with the backbone bond (Table 3). Actually, they are directly related to the opening of the τ' angle.

Since the great value of the intradiad backbone angle is due to the presence of the methyl side-group, this opening

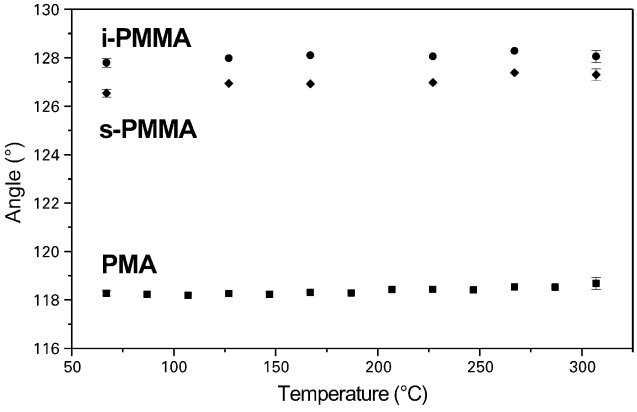

Fig. 4. The intradiad backbone angle, τ', is plotted against temperature for i-PMMA (●), s-PMMA (◆), and PMA (■). For clarity, only standard deviations at 67 and 307 °C are presented.

Table 4
Probabilities of the intradiad rotameric sequence occurrence at 67 °C

Isomer	*tt*	*tg*	$t\bar{g}$	*gg*	$\overline{gg}$	$g\bar{g}$
i-PMMA	0.49	0.22	0.24	0.01	0.01	0.03
s-PMMA	0.61	0.18	0.16	0.03	0.01	0.01

has to be different according to the intradiad rotameric sequence. Table 4 presents the percentage of the rotameric sequences in the intradiad according to a three-state scheme [26] both for the two PMMA configurations and for PMA. The probabilities of *tt* intradiad sequence computed by Vacatello and Flory [24], are 0.77 and 0.23 for syndiotactic and isotactic PMMA chains, respectively, while from MD simulations, they are 0.61 and 0.49, respectively (Table 4). One reason for such differences is that the Theodorou and Suter [7] method for generating a polymer chain leads to differences in the distribution of rotation angles. Moreover, during an MD simulation all the interactions are taken into account. Nevertheless, only intradiad rotameric sequences possessing a trans state, *t*, are considered in our discussion since the probabilities of the other sequences are too low to produce a significant impact on the calculation of the final energy. Table 5 presents for both PMMA configurations the average intradiad backbone angle for the three rotameric sequences possessing at least one trans state. Each intradiad backbone angle whose value is greater than θ_0, 112.67° (Table 1), increases the angle bending energy. The lowest τ' value for the syndiotactic configuration (the minor energy contribution) is obtained when the rotameric sequence is *tt*, while for the isotactic configuration within the same series, it corresponds to the highest value. In the syndiotactic configuration, interactions between the side groups tend to compensate for each other an antiferro-like alignment is observed. In the isotactic configuration, the side chains are placed in a ferro-like alignment. Due to the presence of the methyl groups, the backbone angle has to open in order to counteract the elevated steric repulsions. Such a behavior is not observed in PMA chain since one side-group, the hydrogen atom, is not bulky and consequently, the value of the backbone intradiad angle is low. The high angle energy of the *tt* sequence observed for the meso diad precisely corresponds to the highest probability of appearance of this sequence (49%). This observation is in fact in accordance with the Sundararajan's backbone energy analysis [26]: the highest probability of the *tt* sequence is due to most favorable side-group interaction although the *tt* conformation is higher in energy than *tg* or $t\bar{g}$. It has to be noted that the variation of τ' according to the direction of the COO dipole has been considered. Two directions were privileged: 'up' or 'down' [26]. The up and down configurations correspond to angles of 0 and 180° of the C^2–C^α–C^4–O^1 torsion, respectively. The 0° angle is taken when the carbonyl group eclipses the C^2–C^α bond. As a matter of fact, influences of up–up, down–down, and up–down series, on the value of τ', have been regarded. No distinctions have been observed. The reason is that the direction of the COO dipole does not affect steric repulsions between side-groups.

The introduction of the methyl group implies an enlargement of interchain interactions and intrachain steric repulsions, which result in the aperture of the intradiad backbone angle. From the free-volume theory, both consequences involve an increase in the differentiation between the T_gs of the two PMMA configurations. Such behaviors must also be met in other polymers in the poly(alkyl methacrylate) series, such as PEMA.

In PEMA, the carboxyl side-chain has been elongated by a methyl group compared to PMMA. Such a lengthening increases the overall flexibility and decreases the T_g: the fractional free volume between chains is in fact increased. The density, non-bond and angle bending energies, and the intradiad backbone angle of both PEMA chain tacticities computed at 67 °C are reported in Table 6. The differences between the two PEMA configurations for all these terms are comparable to those obtained between the two PMMA configurations. As a matter of fact, the difference in T_gs between the two configurations is comparable to that between the two PMMA configurations. This is in agreement with what has been experimentally observed by Karasz and MacKnight [21]. These authors indicate that the effect of tacticity on T_g in the poly(alkyl methacrylate) series is strictly an intramolecular effect. From simulation results,

Table 5
Values of the intradiad backbone angle, τ', according to the intradiad rotameric sequence at 67 °C

Intradiad rotameric sequence	s-PMMA (°)	i-PMMA (°)	PMA (°)
$t\bar{g}$	127.8 (±0.1)	127.4 (±0.1)	118.2 (±0.1)
tt	125.8 (±0.1)	128.0 (±0.1)	118.1 (±0.1)
tg	128.2 (±0.1)	127.3 (±0.1)	118.0 (±0.2)

Table 6
Density, energies, and intradiad backbone angle, τ', of the two PEMA chain tacticities at 67 °C

Tacticity	Density (g cm^{-3})	Non-bond (kcal mol^{-1})	Angle bending (kcal mol^{-1})	τ' (°)
Isotactic	0.94 (±0.02)	1621 (±11)	1631 (±13)	127.4 (±0.2)
Syndiotactic	0.90 (±0.02)	1642 (±9)	1582 (±12)	126.6 (±0.1)

this intramolecular effect is observed: it principally comes from a difference in the intradiad backbone angle aperture between the two configurations. However, differences in non-bond interactions between the two chain tacticities are also detected for PMMA and PEMA. Consequently, such interactions contribute to an increase in the differentiation of the T_gs. Actually, this is in accordance with the results obtained by O'Reilly and Mosher [28] who have presented the first lack of constancy of the $\Delta H/RT_g$, where ΔH is the variation of enthalpies at T_g between the iso- and syndiotactic configurations, R is the molar gas constant. This ratio has to be a constant according to Gibbs–DiMarzio model [28].

4. Conclusion

The substitution of an hydrogen atom by a methyl group increases the non-bond interactions as well as the steric repulsions inside the polymer chains. These repulsions lead to an increase in the steric barriers to rotation, and to a significant aperture of the intradiad backbone angle. Such enlargements are different according to the alternation of the side-chains along the backbone chain. For a racemic-diad, non-bond interactions are the most important: this tends to prevent rotations along the s-PMMA chain backbone. For a meso-diad, the intradiad backbone angle aperture is the most significant: the rotations are favored, and mobility along the i-PMMA chain backbone is thus increased. Actually, this aperture acts as an internal plasticization of i-PMMA chains compared with s-PMMA chains. According to the free volume theory, both behaviors tend to increase in both the T_g and the difference in T_gs between the two configurations. Such findings are in accordance with experimental results [27]. Compared with PMA, both enlargements are due to the presence of the methyl group attached to the α-carbon atom. Preliminary simulation studies have shown that the same characteristics are observed when the polystyrene and poly(α-methyl styrene) are simulated.

The greater aperture of the intradiad angle would lead to a greater mobility of the side-chain for the i-PMMA configuration, comparing to the s-PMMA configuration. Such a behavior has recently been confirmed by comparing the local dynamics of both configurations [29]. Actually, Kuebler et al. [17] showed that the side-chain by its rotation implies a greater mobility of the backbone chain. Consequently, a greater mobility of the i-PMMA side-chain affects the backbone-chain mobility more than the s-PMMA one. Consequently, according to the free volume theory the isotactic T_g is lower than the syndiotactic one.

The accurately simulated difference in the T_gs between the two configurations allowed the observation of microscopic phenomena that are in accordance with experimental data and could explain such a difference.

Acknowledgements

I am very grateful to Dr F. Begin for her help in carefully reading the article for English corrections. I also wish to thank Prof. Y. Grohens and Dr D. Mathieu for fruitful scientific discussions.

References

[1] Bashnagel J. J Phys: Condens Matter 1996;8:9599.
[2] Ngai KL. J Phys Chem B 1999;103:5895.
[3] Boyd RH. TRIP 1996;4:12.
[4] Soldera A. Macromol Symp 1998;133:21.
[5] Allen MP, Tildesley DJ. Computer simulation of liquids. Oxford: Clarendon Press, 1987.
[6] Meirovitch H. J Chem Phys 1983;79(1):502.
[7] Theodorou DN, Suter UW. Macromolecules 1985;18:1467.
[8] Rigby D, Roe R-J. J Chem Phys 1987;87:7285.
[9] Parrinello M, Rahman A. J Appl Phys 1981;52:7182.
[10] Andersen HC. J Chem Phys 1980;72:2384.
[11] Haile JM. Molecular dynamics simulation. New York: Wiley, 1992.
[12] Han J, Gee RH, Boyd RH. Macromolecules 1994;27:7781.
[13] Fried JR, Pren P. Comput Theor Polym Sci 1999;9:111.
[14] Burkert U, Allinger NL. Molecular mechanics. Washington: ACS, 1982.
[15] Allinger NL. In: Scheyer PvR, editor. Encyclopedia of computational chemistry. Chichester: Wiley, 1998. p. 1013.
[16] Maple JR, Dinur U, Hagler AT. Proc Natl Acad Sci USA 1988;85:5350.
[17] Sun H. J Phys Chem B 1998;102:7338–64.
[18] Ellys B. Polymers—A property database. Sheffield: Chapman & Hall.
[19] Jensen F. Introduction to computational chemistry. Chichester: Wiley, 1999.
[20] Soldera A. Macromol Symp 1998;133:11.
[21] Karasz FE, MacKnight WJ. Macromolecules 1968;1:537.
[22] Bicerano J. Prediction of polymer properties. New York: Marcel Dekker, 1993.
[23] Gee RH, Boyd RH. Comput Theor Polym Sci 1998;8:91.
[24] Vacatello M, Flory PJ. Macromolecules 1986;19:405.
[25] Plazek DJ, Ngai KL. In: Mark JE, Physical properties of polymers handbook. Woodbury, NY: AIP. p. 139.
[26] Sundararajan PR. Macromolecules 1986;19:415.
[27] O'Reilly JM, Mosher RA. Macromolecules 1981;14:602.
[28] Gibbs JH, DiMarzio SF. J Chem Phys 1958;28:373.
[29] Soldera A, Grohens Y. Macromolecules 2002;35:722.